Available online at www.sciencedirect.com
ScienceDirect
Nuclear Physics B Proceedings Supplement 00 (2014) 1–12
Nuclear Physics B Proceedings Supplement

Probing QCD and hadron physics: highlights of experimental results

Chiara Roda on behalf of the ATLAS, CDF, CMS, D0, H1, ZEUS collaborations

Università and INFN Pisa, Italy

Abstract

The rich set of data collected from HERA, Tevatron and LHC collisions offer an extraordinary possibility to test different aspects of perturbative Quantum Chromodynamics. A selection of recent results illustrates the variety and precision of these tests. The comparison of the experimental data with the most recent theoretical predictions demonstrates the advances made in the theoretical field.

Keywords: QCD, Hadron physics, jet cross section, Boson production

ATL-PHYS-PROC-2014-234
27 October 2014

1. Introduction

The data presently available from hadron and lepton-hadron colliders offer the unique opportunity to test perturbative Quantum Chromodynamics (pQCD) in a new kinematic regime, spanning over many energy scales and in a variety of production modes: electron/positron-proton (ep), proton-antiproton ($p\bar{p}$) and proton-proton (pp) collisions. Experimental tests of pQCD are a fundamental ingredient to understand and verify the strong sector of the Standard Model. Moreover the level of understanding of pQCD and modeling of hadronic physics has direct impact both on precision measurements and on searches for new signals. For instance, the largest systematic uncertainties on the Higgs boson cross section measurement are due to neglected high orders in perturbation theory (scale uncertainties - 8%) and to uncertainties on the Parton Distribution Functions (PDF - 8%) [1]. Jet production or jets in association with vector boson production often constitutes large background processes to searches of new signals or to electro-weak or top-related measurements. Therefore a precise modeling of these processes in a variety of topologies and kinematic ranges increases our capabilities for discovery.

Email address: chiara.roda@cern.ch (Chiara Roda on behalf of the ATLAS, CDF, CMS, D0, H1, ZEUS collaborations)

The abundance of newly available results calls for a selection. The selected results shown in the following are chosen to both give an overview of the different aspect tested in pQCD and to show the impressive precision that the experimental measurements reached.
This paper is organized as follows. A brief summary of the experimental apparatus (accelerators and detectors) related to the results discussed here is given in section 2. Sections 3, 4, 5 and 6 treat selected results on jet cross section, recent advances on PDF and α_s measurements and boson production. The total proton-proton cross section measurement at $\sqrt{s}$ = 7 TeV is discussed in section 7. The summary is given in section 8.

2. The experimental apparatus

The measurements presented here were obtained with data collected at three colliders: HERA, Tevatron and Large Hadron Collider (LHC) [2]. The HERA accelerator operated in the period 1992-2007 colliding electrons/positrons with protons at a center of mass energy between 225 and 319 GeV. The two detectors located at the interaction points of this accelerator, ZEUS [3] and H1 [4], collected an integrated luminosity of 0.5 fb^{-1}/experiment. Tevatron operated between 1987 and 2011 colliding protons with antiprotons at $\sqrt{s}$ = [1.8,1.96] TeV. The total integrated luminosity collected by the D0 [5] and CDF [6] experi-

ments, located on the Tevatron ring, amounts to about 10 fb^{-1}/experiment. LHC started operation in 2009 and completed the first data acquisition period in 2012 collecting proton-proton interactions at $\sqrt{s} = 7$ and 8 GeV. The two general purpose experiments installed at the LHC are ATLAS [7] and CMS [8]. The total integrated luminosities collected by each experiment at $\sqrt{s} = 7$ and 8 GeV are about 5 fb^{-1} and 20 fb^{-1} respectively. The variety of experimental conditions and the differences in the detector technologies and analysis procedures, allow many aspects of pQCD to be tested.

3. Jet cross sections

Collimated jets of hadrons emerging from hadron collisions are the experimental evidence of gluon and quark productions. The high center of mass energy of the LHC collisions allows to study jet production in yet unexplored kinematic ranges, up to the TeV scale. The need to establish a correspondence between observables predicted at parton level and measurements executed at hadron level requires the use of an infrared and collinear safe jet algorithm. Commonly used jet algorithms with these characteristics are the anti-k_t [9] and inclusive k_t [10] algorithms. Unless otherwise stated, the results presented here are obtained with one of these jet algorithms.
CMS and ATLAS studied the inclusive, di-jet, three-jet and multi-jet differential cross sections in many kinematic ranges. Many measurements are also obtained with jets measured with two jet radii. The results are compared to predictions obtained at different perturbative orders and using different PDFs. All these measurements show that pQCD at NLO provides a very good overall description of jet production.

One of the most inclusive jet cross section measurement [11, 12], shown in figure 1, is the double-differential jet spectra for jet radius R=0.7 measured with the CMS detector from pp collisions at $\sqrt{s} = 8$ TeV for p_{T} values varying from 21 GeV up to 2 TeV and rapidity ranging from −4.7 to 4.7. The jet cross section measurement is extended in the low p_{T} region with a data sample of 5.8 pb^{-1} collected with low pile-up conditions. This measurement is compared to NLO pQCD predictions corrected for non-perturbative (NP) effects such as multi-parton interactions and fragmentation effects. The NLO QCD predictions are obtained with NLOJET++ [13] and using NNPDF2.1 PDF set [14]. The cross section spans eleven orders of magnitude with an agreement between data and predictions well within the systematic uncertainties. The Jet Energy Scale (JES) uncertainty dominates the experimental uncertainty, while the theoretical uncertainty is dominated by the PDF uncertainty. The inclusive jet cross section measurement is also compared with theoretical predictions obtained with different PDF sets: CT10 [15], MSTW2008 [16], HERAPDF1.5 [17] and ABM11 [18] each at NLO evolution order. The low p_{T} range is well described by all PDF sets with the only exception of ABM11 one; the p_{T} spectra above few hundred GeV is in agreement only with predictions based on CT10 and NNPDF2.1 sets.

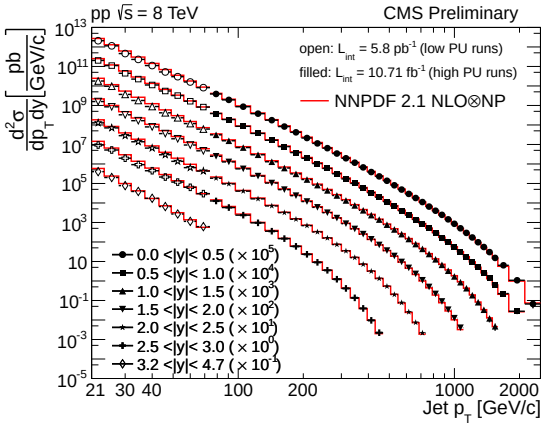

Figure 1: Combined differential inclusive jet cross section as a function of the jet p_{T} and in bins of rapidity as obtained by the CMS collaboration [11, 12]. Open (filled) markers represent measurements obtained with low (high) pile-up data.

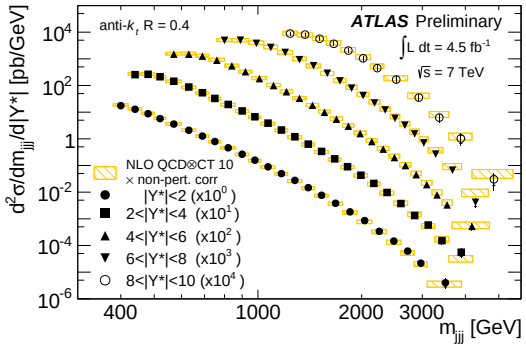

Figure 2: Three-jet double differential cross section as a function of m_{jjj} and binned in $|\mathrm{Y}^*|$ measured by the ATLAS collaboration [19].

Contrary to inclusive jet cross section spectra, multi-

jet cross section spectra are sensitive not only to the jet p_{T} but also to the jet angular distributions. A recent example of this type of measurement is the double-differential three-jet cross section spectra [19] obtained by the ATLAS collaboration with pp collisions at $\sqrt{s}$ = 7 TeV. Jets are measured with radius R=0.4 and R=0.6. The three-jet spectra are shown for R=0.4 in figure 2 as a function of the three-jet invariant mass (m_{jjj}) and of the sum of the absolute rapidity separations between the three leading jets (|Y*|). Invariant masses up to 5 TeV are reached for 8 < |Y*| < 10. The theoretical predictions are obtained at NLO QCD with NLOJET++ convoluted with the CT10 PDF set. Corrections are applied to take into account the hadronisation and the underlying event activity. The renormalisation and factorisation scales are set equal to the mass of the three-jet system. The NLO predictions with the CT10 PDF correctly describe the three-jet double differential spectra that spans over almost seven orders of magnitude. NLO predictions are also obtained for the HERAPDF1.5, MSTW2008, NNPDF2.3 [20], GJR08 [21], ABM11 PDF sets. A good agreement is observed with all the PDF sets with the only exception of the prediction based on the ABM11 set that exhibits a tension with data in almost the whole kinematic region. The ratios of NLO QCD predictions obtained with different PDF sets, to data as a function of m_{jjj}, binned in |Y*| are shown in figures 3(a). Only the comparison with CT10, MSTW2008 and HERAPDF1.5 are shown, the complete set of ratios can be found in Reference [19]. The data to theoretical predictions ratio for R=0.6p are shown in figure 3(b). While NLO predictions correctly describe the data for a jet radius R=0.4 at R=0.6 the predictions underestimate the data by approximately 15%. The result is independent of the PDF set, therefore is not due to assumptions made in different PDF determinations.

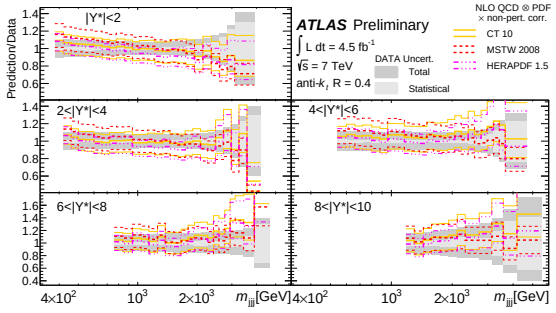

(a)

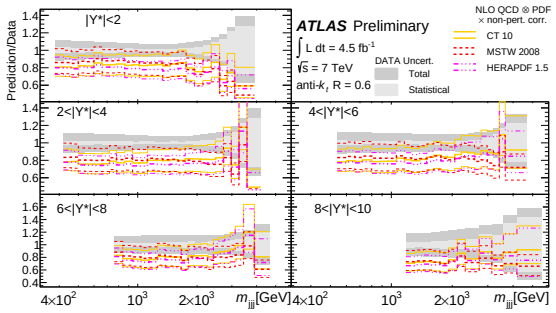

(b)

Figure 3: Ratio of NLO QCD predictions, obtained with NLOJET++ with different PDF sets (CT10, MSTW2008, HERAPDF1.5) and corrected for non-perturbative effects, to data as a function of m_{jjj} and binned in |Y*| obtained by ATLAS [19]. The ratios are shown for jets reconstructed with the anti-k$_t$ algorithm with R=0.4 (3(a)) and R=0.6 (3(b)). The thick line shows the central value and the thin lines represent the total theory uncertainty.

The effect of the choice of the jet radius on the cross section measurement is reported by the CMS collaboration [22]. In this study the ratio $\mathcal{R}(0.5, 0.7)$ defined as:

$$\left(\frac{\mathrm{d}\sigma^{0.5}}{\mathrm{d}p_{\mathrm{T}}} - \frac{\mathrm{d}\sigma^{0.7}}{\mathrm{d}p_{\mathrm{T}}}\right) \Big/ \left(\frac{\mathrm{d}\sigma^{0.7}}{\mathrm{d}p_{\mathrm{T}}}\right) = \mathcal{R}(0.5, 0.7) - 1. \qquad (1)$$

has been measured as a function of the jet p_{T}. This variable is sensitive to perturbative radiation, hadronisation effects and underlying event activity. The variable $\mathcal{R}(0.5, 0.7)$ is shown in figure 4 for six bins of rapidity as a function of the jet p_{T}. The jet radius ratio does not exhibit a significant rapidity dependence. The ratio rises toward unity with increasing p_{T}. In figure 4(a) the data are compared to various predictions to investigate the effect of different perturbative orders and of non-perturbative effects. The NLO predictions are obtained using the technique discussed in Reference [23]. The different curves show how NP effects are significant for p_{T}< 1 TeV. However, even including NP effects, the fixed order NLO predictions tend to overestimate $\mathcal{R}(0.5, 0.7)$ in most kinematic regions. A better description is obtained when using predictions obtained with POWHEG [24] interfaced to PYTHIA6 [25] (figure 4(a)). In this case the combination of NLO predictions interfaced to parton shower Monte Carlo (MC) better model the data.

4. Recent advances in PDF determination

The PDF uncertainty is often one of the largest contribution to the theoretical precision of hadron production

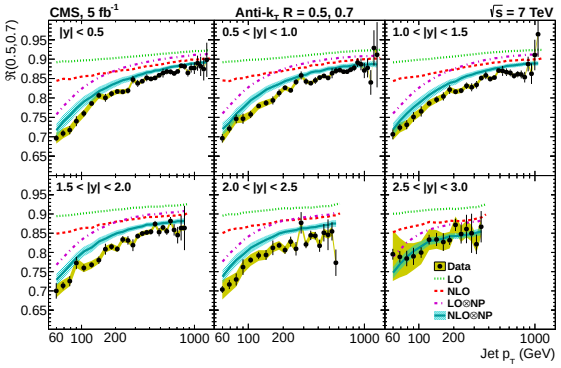

(a)

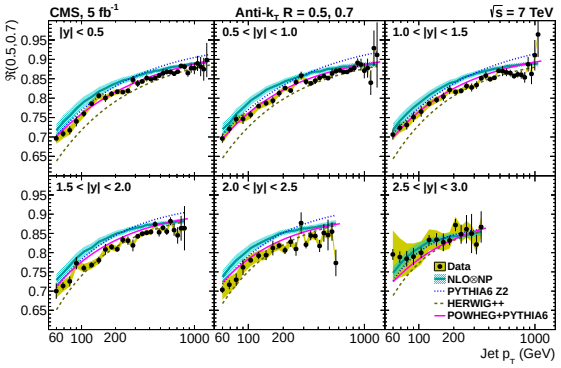

(b)

Figure 4: Cross section ratio $\mathcal{R}(0.5, 0.7)$ (see text for the definition) in six rapidity bins as a function of jet p_T. In figure 4(a) data are compared to LO and NLO prediction with and without non perturbative (NP) corrections applied. In figure 4(b) data are compared to different predictions. The error bars on the data points represent the statistical and the uncorrelated systematic uncertainty added in quadrature, and the shaded bands represent the correlated systematic uncertainty. The NLO calculations are provided by G.Soyez [23].

processes. Recently the H1 and ZEUS collaborations produced new NLO and NNLO PDF sets named HERAPDF2.0 [26]. These new sets are based on neutral and charged current $e^{\pm}p$ inclusive cross sections obtained from the full HERAI and HERAII datasets. The larger HERAII data set allows a significant improvement in the precision of the cross section measurements at high x and Q^2. A comparison of the new HERAPDF2.0 set with the HERAPDF1.5 set is shown in figure 5. While the shapes for the two sets are similar, the new gluon and sea PDF have smaller uncertainties both at low and high x. The new valence quark PDF also shows a reduced uncertainty at high x. The available PDF sets do not cover the full phase space available at LHC there-

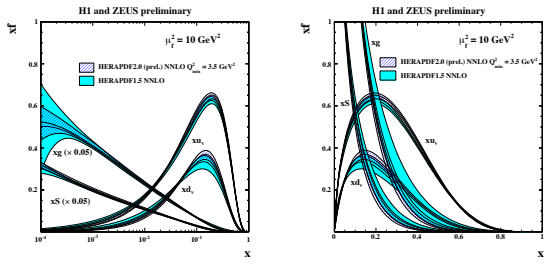

(a) (b)

Figure 5: HERAPDF2.0 (NNLO) parton distribution functions for xu_v, xd_v, $xS = 2x(\overline{U}+\overline{D})$, xg at the scale $\mu_f^2 = 10\,\mathrm{GeV}^2$, for the $Q^2_{\mathrm{min}} = 3.5\,\mathrm{GeV}^2$ fit compared to HERAPDF1.5 (NNLO) on log (a) and linear (b) scales. The bands represent the total uncertainties.

fore predictions, in the LHC phase space, are based on extrapolations that are affected by large uncertainties. A typical example is the large spread of the gluon PDF values predicted by different PDF sets (figure 6), not covered by the PDF uncertainty, in many kinematic regions. This situation can be improved by adding information from the LHC measurements for the PDF determination. A recent example [28] is the use of CMS inclusive

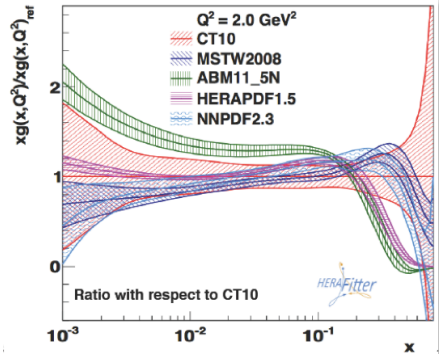

Figure 6: Ratios of gluon parton distribution functions to CT10 PDF [27].

jet cross section measurement at $\sqrt{s} = 7$ TeV [29] to the data used to determine the HERAPDF1.0 PDF set. This study is done using the HERAFitter [27] framework. The gluon PDF determined with this additional data (figure 7) is slightly harder than the gluon PDF obtained from deep inelastic scattering data only. Moreover the fractional uncertainty on the gluon PDF is significantly reduced at $x > 0.01$. Part of the fractional uncertainty reduction is however due to the higher PDF

values. The precision of the measurement at low x is systematically limited since it is dominated by low p_T jets affected by a large energy scale uncertainty.

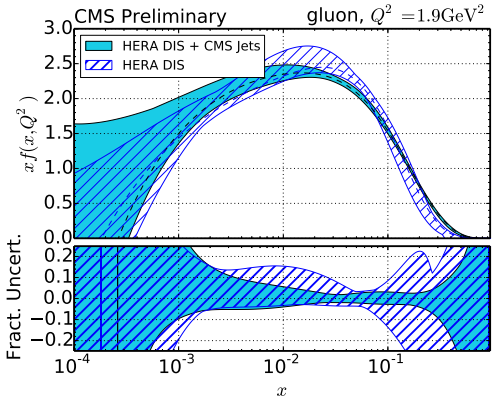

Figure 7: Gluon PDF as a function of x as derived from HERA inclusive DIS data alone (hatched blue) and in combination with CMS inclusive jet data from 2011 (light blue) [28]. The PDF are shown at the starting scale of $Q^2 = 1.9$ GeV^2. Only the total uncertainty of the PDF is shown.

5. Recent updates on the determination of the strong coupling constant at hadron colliders

Beside the quark masses, the only other free parameter in the QCD Lagrangian is the strong coupling constant α_S which is a quantity that enters in theoretical predictions in the context of perturbation theory. The world average value of $\alpha_S(M_Z)$, obtained from (at least) NNLO QCD calculations is $\alpha_S(M_Z) = 0.1185 \pm 0.0005$ [30] and reaches a precision of better than 1%. This value is dominated by measurements based on lattice QCD calculations. A compilation of the most recent $\alpha_S(M_Z)$ measurements obtained at hadron colliders is shown in figure 8. The latest determination of $\alpha_S(M_Z)$ obtained with LHC data has been derived by CMS using the inclusive jet cross section measured at $\sqrt{s} = 7$ TeV [28]. The $\alpha_S(M_Z)$ value obtained with CT10-NLO PDF is:

$$\alpha_S(M_Z) = 0.1185 \pm 0.0019\ (\text{exp.}) \pm 0.0028\ (\text{PDF})$$
$$\pm 0.0008\ (\text{NP})\ ^{+0.0055}_{-0.0022}\ (\text{scale}).$$

The overall precision is about 5% with the largest contribution to the uncertainty given by the neglected perturbative orders.
The H1 collaboration has also recently published an analysis to extract $\alpha_S(M_Z)$ from inclusive and multi-jet cross sections. The best precision is reached from the fit to normalized multi-jet cross sections and is [31]:

$$\alpha_S(M_Z) = 0.1165 \pm 0.0008\ (\text{exp.}) \pm 0.0038\ (\text{PDF, theo})$$

The precision of the measurement is limited by the theoretical uncertainties but it is interesting to note that the experimental precision is 0.7%.

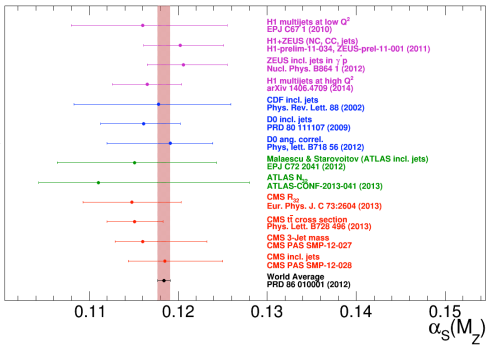

Figure 8: Compilation of recent $\alpha_S(M_Z)$ measurements obtained at hadron colliders [32]. The world average value is also indicated. The CMS value illustrated in this paper is the one just above the world average value while the H1 value is the fourth from the top.

All $\alpha_S(M_Z)$ values obtained from hadron collider data are consistent with the world average (figure 8) however they are affected by quite large uncertainties. The very interesting information obtained from hadron collider data is the measurement of the α_S energy dependence. Thanks to the results collected at the Tevatron and LHC, the $\alpha_S(Q)$ measurement is extended up to few TeV as is shown in figure 9. The distribution is in full agreement with the QCD prediction of Asymptotic Freedom.

6. Boson production

The measurement of vector boson production in association with jets allows QCD predictions to be tested with the additional feature of a clean uncolored probe that emerges from the parton-parton scattering. This measurement is also sensitive to quark PDF. Moreover, as stated above, often these processes are sizable backgrounds to searches or to precision measurements and it is therefore important to understand the level at which they are predictable.

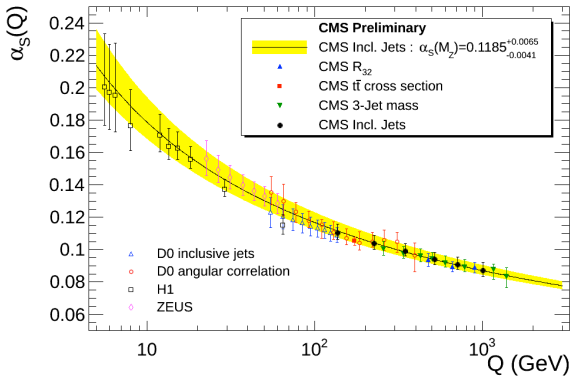

Figure 9: Measurement of the α_s energy dependence as obtained from hadron collider measurements [32].

6.1. Photon production

The measurement of the differential distributions of prompt isolated photons has been obtained from $\sqrt{s}$ = 7 TeV pp collisions collected with the ATLAS detector. This measurement [33] tests the different production mechanism of prompt photons: Compton, annihilation and fragmentation. The predicted fractional contribution depends both on the center of mass energy of the pp ($p\overline{p}$) collisions and on the photon transverse energy (E_T^γ). The cross section as a function of E_T^γ is shown in figure 10(a). It extends up to E_T^γ=1 TeV and changes by more than five orders of magnitude. The data are well described by the NLO predictions obtained with JETPHOX [34] and using the CT10 PDF set. The predictions of the LO parton-shower MC generators, PYTHIA6 and HERWIG [35], are also shown. The PYTHIA6 model describes the data fairly well, while HERWIG falls below the data by 10%-20%. The shapes of the cross sections are well described by both models. The data are also compared to MC predictions that include only direct photons from qg → qγ and qq → gγ processes calculated at LO QCD. Figure 10(b) shows that in this case the prediction at low E_T^γ is about 20% lower than data. The correct inclusion of fragmentation processes is therefore fundamental to correctly predict the shape of the spectra.

The first measurement [36] of photon production at $\sqrt{s}$ =8 TeV has been obtained by CMS and it is shown in figure 11. The large data set allows to halve the statistical uncertainty. Data are compared to LO predictions and, as expected, fail to describe the spectra. Work is on-going to obtain a comparison with NLO predictions.

The D0 collaboration has recently published the mea-

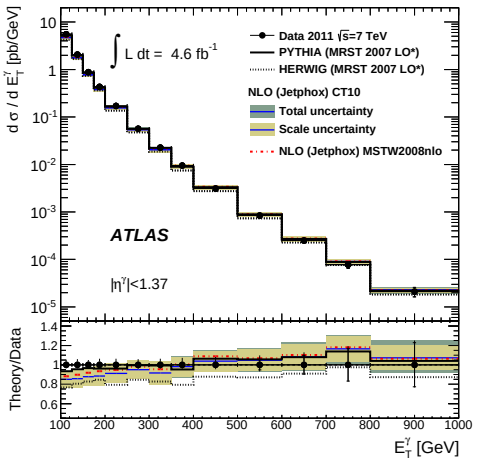

(a)

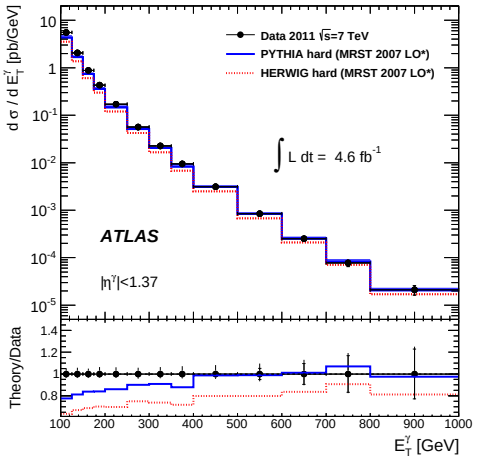

(b)

Figure 10: (a) Measured and predicted inclusive prompt photon cross section as a function E_T^γ with the ATLAS detector at $\sqrt{s}$ = 7 TeV [33]. The inner error bars on the data points show statistical uncertainties, while the full error bars show statistical and systematic uncertainties added in quadrature. The bottom panel shows the corresponding theory/data ratio, in which the data points are centered at one. (b) Same data as in (a) but the comparison is made with MC predictions that include only direct photons from the hard processes.

surement of the production of photons in association with one or two b-jets [37]. This study is interesting not only as a QCD test but also because it can give access to the b-quark PDF. In this case jets are reconstructed with the Run II cone algorithm [38] with cone radius R = 0.5. The differential cross section of photons produced in association with two b-jets as a function of the photon transverse energy is show in Figure 12. Both the NLO QCD calculation and the prediction obtained with the k_T-factorisation [39] approach are in agreement with the data. On the contrary SHERPA [40] and PYTHIA6 fails, at different levels, to describe the whole distribution.

6.2. *W and Z boson production in association with light flavor jets*

The large sample of pp collisions collected by ATLAS and CMS at $\sqrt{s}$ =7 TeV has allowed a very detailed investigation of the production of the W and Z boson in association with jets. In particular both CMS and ATLAS have recently reported a very detailed study of the W+jet differential cross sections for different jet multiplicities and as a function of many variable [41, 42]. For instance the differential cross sections are measured as a function of the sum of the transverse momentum of the jets, of the jet angular separation, of the invariant mass of the two jets with the highest transverse momenta and of the sum of the transverse momenta of the jets, lepton and neutrino. Differential cross sections for jet multiplicity up to five jets are also studied. The measurements are compared to NLO pQCD calculations, resummation calculations and to predictions from different Monte Carlo generators implementing NLO and LO matrix elements supplemented by parton showers. As illustration of these studies the cross sections of the W boson in association with jets as a function of the jets multiplicity, as obtained by ATLAS and CMS are shown in figures 13 and 14 respectively. The data are well reproduced by the different predictions over five orders of magnitude. The overall conclusion that can be drawn by these detailed study is that the best description of the cross sections is given by NLO predictions interfaced to parton showers such as BLACKHAT+SHERPA with some exception for variables such as the scalar sum of the p_T of all identified jets or all identified objects.

Recently the double differential cross section of the production of the Z boson in association with jets has been measured in pp collisions at $\sqrt{s}$ =8 TeV with the CMS detector [50]. The cross section is measured as a function of the leading jet transverse momentum and rapidity. Jets are measured for transverse momenta ranging

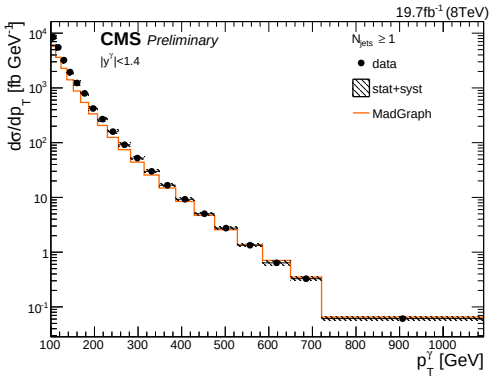

Figure 11: The γ differential transverse momentum cross-section in an inclusive γ+jets, $n_{jets} \geq 1$ selection for central rapidities $|y_\gamma| < 1.4$ in data compared with prediction from MADGRAPH+PYTHIA6 obtained from $\sqrt{s}$ = 8 TeV pp collisions with CMS detector [36].

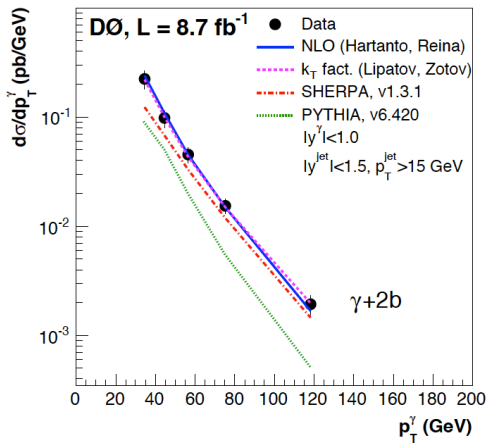

Figure 12: The γ+2 b-jet differential production cross sections as a function of E_T^γ obtained from $p\bar{p}$ collisions with the D0 detector [37]. The uncertainties on the data points include statistical and systematic contributions. The measurements are compared to the NLO QCD calculations using the CTEQ6.6M PDFs (solid line). The predictions from SHERPA, PYTHIA6 and the k_T factorisation approach are also shown.

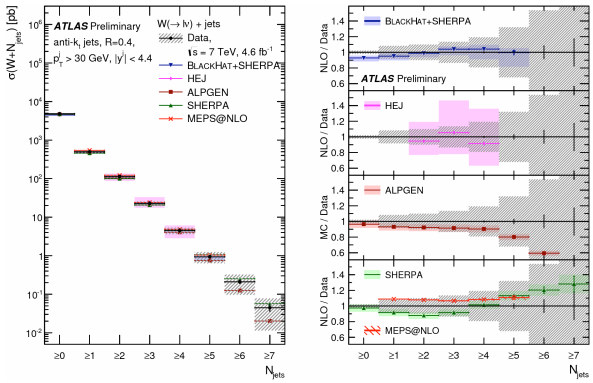

Figure 13: W+jets cross section as a function of the inclusive jet multiplicity obtained by ATLAS [41]. For the data, the statistical uncertainties are shown by the vertical bars, and the combined statistical and systematic uncertainties are shown by the black-hashed regions. The data are compared to predictions from BLACKHAT+SHERPA [43, 44, 45], HEJ [46], ALPGEN [47], SHERPA [40] and MEPS@NLO [48]. The left-hand figure shows the differential cross sections and the right-hand figure shows the ratios of the predictions to the data.

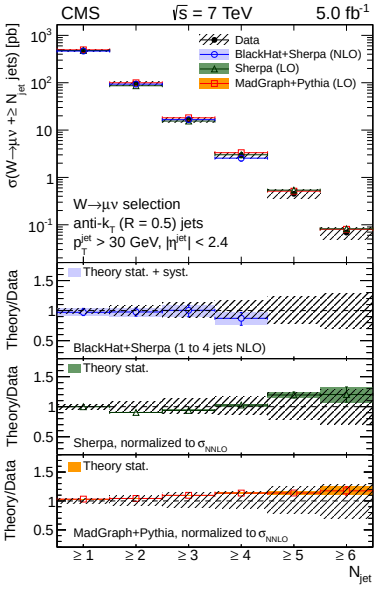

Figure 14: W+jets cross section as a function of the inclusive jet multiplicity, obtained by CMS [42], compared to the predictions of MADGRAPH [49] + PYTHIA, SHERPA, and BLACKHAT+ SHERPA. Black circular markers with the grey hatched band represent the data measurement and their uncertainty. Overlaid are the predictions together with their statistical uncertainties. The lower plots show the ratio of each prediction to the unfolded data.

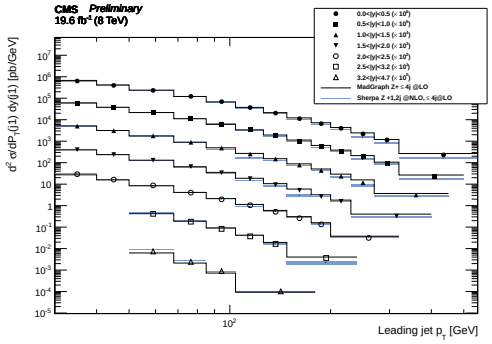

Figure 15: Double differential cross section versus leading jet transverse momentum for various rapidity bins in the di-muon channel measured by CMS in pp collisions at $\sqrt{s}$ = 8 TeV [50]. Data points are shown with statistical error bars. The black lines indicate MADGRAPH predictions normalized to the inclusive NNLO cross-section. The SHERPA predictions are shown as blue bands, whose thickness indicates the statistical uncertainty.

from 40 to 550 GeV and for rapidity up to |4.7|. Theoretical predictions are obtained both with SHERPA and MADGRAPH interfaced to PYTHIA6 normalized to the NNLO cross section. The double differential cross section is shown in figure 15. The MADGRAPH predictions tend to overestimate the data at $p_T > 100$ GeV roughly independently of the jet rapidity. An overall agreement is seen between SHERPA predictions and the data with the exception of some rapidity and p_T regions that need a further investigation.

6.3. *W and Z boson production in association with heavy flavor jets*

The differential and total production cross sections of the W boson in association with a charm quark have been recently studied in pp collision at $\sqrt{s}$ = 7 TeV by ATLAS [51] and CMS [52]. The W+c production at LO proceeds mainly through the gs → Wc diagram, while the similar diagram gd → Wc is Cabibbo suppressed and contributes only about 10%. This process is therefore sensitive to the s-quark PDF. The amount of s- quark suppression with respect of the light-quark sea varies in different PDF depending on the choice of the data set used to obtain the PDF itself. A quite large spread among s-quark PDF sets is observed as shown in figure 16. A comparison of the W+c production cross section obtained by ATLAS and CMS with various PDF sets is shown in figure 17. Considering the large experimental and theoretical uncertainties the measurement

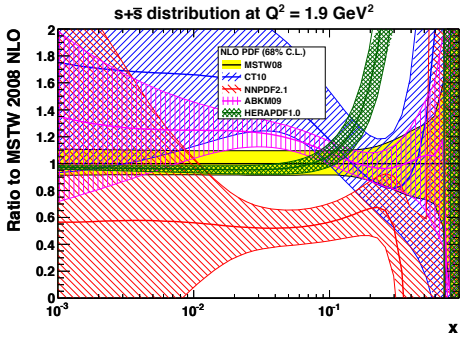

Figure 16: Ratio of various strange-quark PDF sets to the MSTW 2008 strange PDF [53, 54]

are all in agreement with predictions however a small tension is observed between the ATLAS and CMS results. In fact ATLAS data, contrary to CMS data, seems to favor the s-quark PDF where the s-sea is not suppressed with respect to the light-quark sea (ATLAS-epWZ12 [55] and NNPDF2.3coll [20]). Reduced theoretical and experimental uncertainties are needed for a more definite statement on this point.

The CDF collaboration also presented new results on the associated production of W bosons and charm [58] in $p\bar{p}$ collisions at $\sqrt{s} = 1.96$ TeV. The production ratio $\sigma(W + D^*)/\sigma(W)$ has been measured in the W leptonic decay channel using full D^* reconstruction as a function of the $p_T(D^*)$. The measurement, shown in figure 18, extends down to $p_T(D^*) = 3$ GeV. The data are well described by the prediction obtained with PYTHIA6 interfaced to CTEQ5L PDF set. The measurement is statistically limited.

Another interesting result that has recently become available is the study of the differential Z+b-jet cross-section obtained from the ATLAS collaboration in pp collisions at $\sqrt{s} = 7$ TeV [59]. A detailed study of Z +1 b-jet and Z + 2 b-jets topologies is obtained and compared to theoretical pQCD calculations. NLO predictions obtained with MCFM and aMC@NLO provide the best overall description of the data. This process is also interesting since it can discriminate between the four-flavour number scheme (4FNS), which only considers parton densities from gluons and the first two quark generations in the proton and the five-flavour number scheme (5FNS), which allows a b-quark density in the initial state. In a calculation to all orders, the 4FNS and 5FNS methods must give identical results; however, at a given order, differences can occur between the schemes [60].

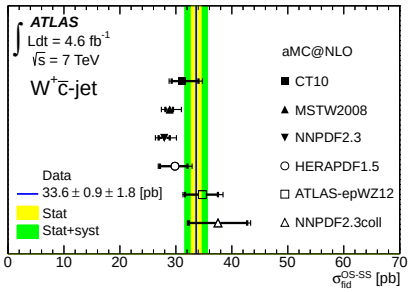

(a)

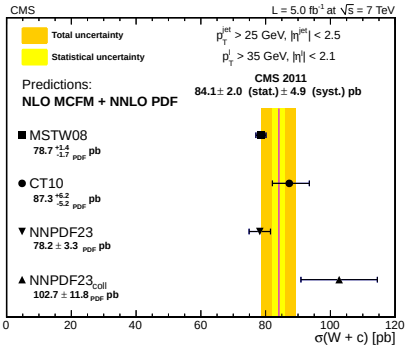

(b)

Figure 17: (a) Measured $W^+\bar{c}$ fiducial cross section [51] obtained from the ATLAS experiment compared to various PDF predictions based on aMC@NLO [56]. (b) Measured W+c cross section [52] obtained from the CMS experiment compared to various PDF predictions based on MCFM [57].

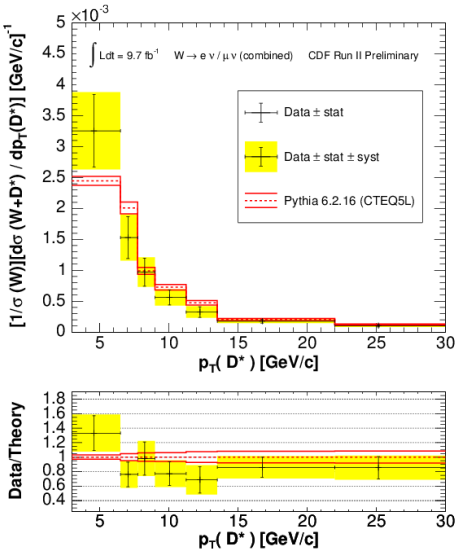

Figure 18: The ratio of $\sigma(\mathrm{W} + \mathrm{D}^*)/\sigma(\mathrm{W})$ as a function of $p_{\mathrm{T}}$for electron and muon channel. The ratio of the simulated distribution to data is shown in the lower panels.

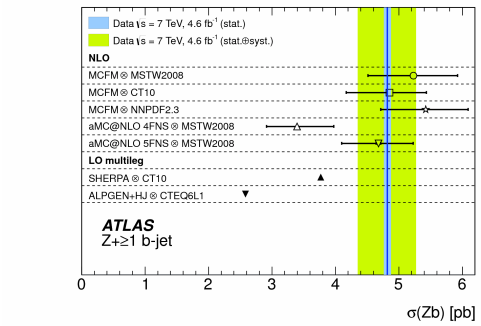

(a)

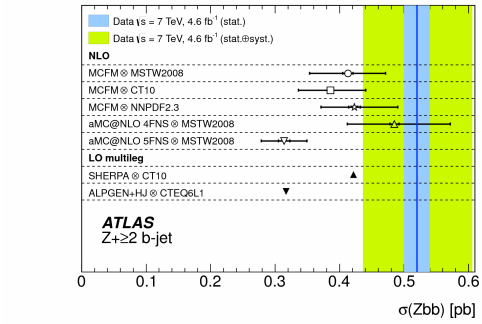

(b)

Figure 19: Total fiducial cross-sections for (a) Z + 1 b-jet, and (b) Z + 2 b-jets obtained pp collisions at $\sqrt{s}$ = 7 TeV with the ATLAS detector [59]. Data are compared is to NLO predictions from MCFM interfaced to different PDF sets and aMC@NLO interfaced MSTW 2008 set in both the 4FNS and 5FNS. Comparisons are also made to LO multi-legged.

Recently, a full particle-level prediction at NLO in the 4FNS with matched parton shower [60] has become available, and can be extended to a 5FNS prediction as well. The differences in between these calculations give a range of theoretical predictions for the total Z + 1 b-jet and Z + 2 b-jet cross sections that are compared with data in figure 19. NLO predictions from MCFM and aMC@NLO generally provide the best overall description of the data. The aMC@NLO prediction with data differs in the Z + 1 b-jet and Z + 2 b-jets cases. The former is better described by the 5FNS prediction while the latter is better described by the 4FNS prediction. The predictions, even at NLO, are dominated by the scale uncertainty therefore more conclusive statements need predictions at higher orders.

7. Total proton-proton cross section measurement at $\sqrt{s}$ = 7 TeV

The measurement of the total pp cross section has been recently obtained by the ATLAS collaboration using the ALFA sub detector [61]. The measurement is based on the classic method that uses the optical theorem and the elastic scattering in the forward direction to calculate the total cross section. An independent measurement of the luminosity is needed and this is accomplished with Van Der Meer scans. The analysis allows to obtain the total and elastic cross sections and from these ones, by subtraction, the inelastic cross section. The cross sections are:

$$\sigma_{\mathrm{tot}}(\mathrm{pp} \to \mathrm{X}) = 95.35 \pm 1.36 \text{ mb}$$
$$\sigma_{\mathrm{el}}(\mathrm{pp} \to \mathrm{pp}) = 24.00 \pm 0.60 \text{ mb}$$
$$\sigma_{\mathrm{inel}}(\mathrm{pp} \to \mathrm{pp}) = 71.34 \pm 0.90 \text{ mb}$$

The measured total pp cross section is compared in figure 20 to results obtained from the TOTEM experiment, low energy experiments and cosmic ray experiments (see [61] and references therein).

8. Summary

The data available from HERA, Tevatron and LHC allow to test the pQCD predictions in a new kinematic

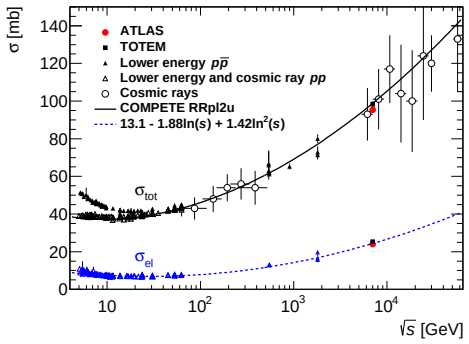

Figure 20: Total and elastic cross-section measurements obtained from ATLAS and from other experiments (see [61] and references therein) overlaid with model predictions as a function of the center of mass energy.

region and with exclusive and inclusive measurements. For many processes differential or double differential measurements are obtained. Both on the experimental and theoretical side many advances were made. In many measurements an experimental uncertainty at the same level, or better, than the theoretical uncertainty is reached and new tools for predictions have become available. These tools provide a reliable and improved description of data for most of the measurements and at the same time they offer increased flexibility. The LHC data proved the α_S running up to TeV scale and many measurements have reached the precision needed to contribute to the PDF extraction. The solid ground provided by all these tests constitute the starting point for further investigations at even higher energy with the soon coming $\sqrt{s} = 13$ TeV LHC data.

References

[1] ATLAS Collaboration, Phys.Lett. B738 (2014) 68–86. arXiv:1406.7663, doi:10.1016/j.physletb.2014.09.008.

[2] LHC Collaboration, JINST 1 (2008) S08001. doi:10.1088/1748-0221/3/08/S08001.

[3] ZEUS Collaboration Status Report, DESY - http://www-zeus.desy.de/bluebook/bluebook.html.

[4] H1 Collaboration, Nucl.Instrum.Meth. 386 (23) (1997) 310. doi:http://dx.doi.org/10.1016/S0168-9002(96)00893-5.

[5] V. Abazov, et al., Nucl.Instrum.Meth. A565 (2006) 463–537. arXiv:physics/0507191, doi:10.1016/j.nima.2006.05.248.

[6] CDF Collaboration, Phys. Rev. D 71 (2005) 052003. doi:10.1103/PhysRevD.71.052003.

[7] ATLAS Collaboration, JINST 3 (2008) S08003. doi:10.1088/1748-0221/3/08/S08003.

[8] CMS Collaboration, JINST 4 (2008) S08004. doi:10.1088/1748-0221/3/08/S08004.

[9] M. Cacciari, G. P. Salam, G. Soyez, JHEP 0804 (2008) 063. arXiv:0802.1189, doi:10.1088/1126-6708/2008/04/063.

[10] S. D. Ellis, D. E. Soper, Phys.Rev. D48 (1993) 3160–3166. arXiv:hep-ph/9305266, doi:10.1103/PhysRevD.48.3160.

[11] CMS Collaboration CMS-PAS-SMP-12-012 - http://cdsweb.cern.ch/record/1547589.

[12] CMS Collaboration CMS-PAS-FSQ-12-031 - http://cdsweb.cern.ch/record/1564932.

[13] Z. Nagy, Phys. Rev. D68 (2003) 094002.

[14] R. D. Ball, L. D. Debbio, S. Forte, A. Guffanti, J. I. Latorre, J. Rojo, M. Ubiali, Nuclear Physics B 838 (12) (2010) 136 – 206. doi:http://dx.doi.org/10.1016/j.nuclphysb.2010.05.008.

[15] H. L. Lai, et al., Phys. Rev. D82 (2010) 074024. arXiv:1007.2241, doi:10.1103/PhysRevD.82.074024.

[16] A. Sherstnev, R. S. Thorne C55 (2008) 553. arXiv:0711.2473.

[17] H1 and ZEUS Collaborations, JHEP 2010 (1). doi:10.1007/JHEP01(2010)109.

[18] S. Alekhin, J. Blümlein, S. Moch, Phys. Rev. D 86 (2012) 054009. doi:10.1103/PhysRevD.86.054009.

[19] ATLAS Collaboration ATLAS-CONF-2014-045 - https://cds.cern.ch/record/1741019.

[20] R. D. Ball, V. Bertone, S. Carrazza, C. S. Deans, L. Del Debbio, et al., Nucl.Phys. B867 (2013) 244–289. arXiv:1207.1303, doi:10.1016/j.nuclphysb.2012.10.003.

[21] M. Glűck, P. Jimenez-Delgado, E. Reya, C. Schuck, Physics Letters B 664 (12) (2008) 133 – 138. doi:http://dx.doi.org/10.1016/j.physletb.2008.04.063, [link].
URL http://www.sciencedirect.com/science/article/pii/S0370269308005364

[22] CMS Collaboration CMS-SMP-13-002, CERN-PH-EP-2014-068. arXiv:1406.0324.

[23] G. Soyez, Phys.Lett. B698 (2011) 59–62. arXiv:1101.2665, doi:10.1016/j.physletb.2011.02.061.

[24] S. Alioli, P. Nason, C. Oleari, and E. Re, JHEP 1006 (2010) 043. arXiv:1002.2581.

[25] T. Sjostrand, S. Mrenna, P. Z. Skands, JHEP 0605 (2006) 026. arXiv:hep-ph/0603175, doi:10.1088/1126-6708/2006/05/026.

[26] HERAFitter Group- http://www.herafitter.org.

[27] H1 and ZEUS Collaborations ZEUS-prel-14-007, H1prelim-14-042 - http://www-h1.desy.de/psfiles/confpap/DIS2014/H1prel-14-042.pdf.

[28] CMS Collaboration CMS-PAS-SMP-12-028 - http://cdsweb.cern.ch/record/1564932.

[29] CMS Collaboration, Phys. Rev. D 87 (2013) 112002. doi:10.1103/PhysRevD.87.112002.

[30] K.A. Olive et al. (Particle Data Group), Chin. Phys. C 38 (2014) 090001.

[31] H1 Collaboration DESY-14-089. arXiv:1406.4709.

[32] CMS Collaboration http://twiki.cern.ch/twiki/bin/view/CMSPublic/PhysicsResultsSMP#Strong_coupling_results.

[33] ATLAS Collaboration, Phys. Rev. D 89 (2014) 052004. doi:10.1103/PhysRevD.89.052004.

[34] P. Aurenche et al., Phys. Rev. D73 (2006) 094007. doi:10.1103/PhysRevD.73.094007.

[35] G. Corcella et al., JHEP 0101 (2001) 010. doi:10.1088/1126-6708/2001/01/010.

[36] CMS Collaboration - CMS-PAS-SMP-14-005 - 2014/7 - http://cds.cern.ch/record/1740969.

[37] D0 Collaboration FERMILAB-PUB-14-135-E. arXiv:1405.3964, doi:10.1016/j.physletb.2014.09.007.
[38] G. C. Blazey, J. R. Dittmann, S. D. Ellis, V. D. Elvira, K. Frame, et al. (2000) 47–77arXiv:hep-ex/0005012.
[39] F. V. Lipatov, N. P. Zotov, J. Phys. G 34 (2007) 219.
[40] T. Gleisberg, et al., JHEP 0902 (2009) 007. arXiv:0811.4622, doi:10.1088/1126-6708/2009/02/007.
[41] ATLAS Collaboration - CERN-PH-EP-2014-177. arXiv:1408.5778.
[42] CMS Collaboration - CMS-SMP-12-023, CERN-PH-EP-2014-134. arXiv:1406.7533.
[43] J. Alcaraz Maestre, et al.arXiv:1203.6803.
[44] C. Berger, Z. Bern, L. J. Dixon, F. Febres Cordero, D. Forde, et al., Phys.Rev. D80 (2009) 074036. arXiv:0907.1984, doi:10.1103/PhysRevD.80.074036.
[45] C. Berger, Z. Bern, L. J. Dixon, F. Febres Cordero, D. Forde, et al., Phys.Rev.Lett. 106 (2011) 092001. arXiv:1009.2338, doi:10.1103/PhysRevLett.106.092001.
[46] T. G. et al., JHEP 0302 (2003) 056. 28 p. arXiv:hep-ph/0311263.
[47] M. L. Mangano, M. Moretti, F. Piccinini, R. Pittau, A. D. Polosa, JHEP 0307 (2003) 001. arXiv:hep-ph/0206293.
[48] S. Hoeche, F. Krauss, M. Schonherr, F. Siegert, JHEP 1304 (2013) 027. arXiv:1207.5030, doi:10.1007/JHEP04(2013)027.
[49] J. Alwall, M. Herquet, F. Maltoni, O. Mattelaer, T. Stelzer, JHEP 1106 (2011) 128. arXiv:1106.0522, doi:10.1007/JHEP06(2011)128.
[50] CMS Collaboration CMS-PAS-SMP-14-009 - http://cds.cern.ch/record/1728345.
[51] ATLAS Collaboration , JHEP 1405 (2014) 068. arXiv:1402.6263, doi:10.1007/JHEP05(2014)068.
[52] CMS Collaboration, JHEP 1402 (2014) 013. arXiv:1310.1138, doi:10.1007/JHEP02(2014)013.
[53] J. Abelleira Fernandez, et al., J.Phys. G39 (2012) 075001. arXiv:1206.2913, doi:10.1088/0954-3899/39/7/075001.
[54] Private communication from Graeme Watt.
[55] S. Frixione, E. Laenen, P. Motylinski, B. R. Webber, C. D. White, JHEP 07 (2008) 029. arXiv:0805.3067, doi:10.1088/1126-6708/2008/07/029.
[56] R. Frederix, S. Frixione, V. Hirschi, F. Maltoni, R. Pittau, et al., Phys.Lett. B701 (2011) 427–433. arXiv:1104.5613, doi:10.1016/j.physletb.2011.06.012.
[57] J. M. Campbell, R. K. Ellis, Phys. Rev. D60 (1999) 113006. arXiv:hep-ph/9905386, doi:10.1103/PhysRevD.60.113006.
[58] CDF Collaboration, CDF Note 11087 - http://www-cdf.fnal.gov/physics/new/qcd/.
[59] ATLAS Collaboration - CERN-PH-EP-2014-118. arXiv:1407.3643.
[60] F. Maltoni, G. Ridolfi, M. Ubiali, JHEP 1207 (2012) 022. arXiv:1203.6393, doi:10.1007/JHEP04(2013)095,10.1007/JHEP07(2012)022.
[61] ATLAS Collaboration - CERN-PH-EP-2014-177. arXiv:1408.5778.